ARTICLE

High-resolution Infrared Spectroscopy of $^{15}N_2^{16}O$ in 1650−3450 cm$^{-1\dagger}$

Jun-he Du[a], An-wen Liu[a]*, V. I. Perevalov[c], S. A. Tashkun[c], Shui-ming Hu[a,b]*

a. Department of Chemical Physics, University of Science and Technology of China, Hefei 230026, China
b. Hefei National Laboratory for Physical Sciences at Microscale, University of Science and Technology of China, Hefei 230026, China
c. Laboratory of Theoretical Spectroscopy, V. E. Zuev Institute of Atmospheric Optics SB, Russian Academy of Science, 1, Akademician Zuev sq., 634021, Tomsk, Russia

High-resolution ro-vibrational spectroscopy of $^{15}N_2^{16}O$ in 1650−3450 cm^{-1} region is studied using highly enriched isotopologue sample. The positions of more than 7300 lines of $^{15}N_2^{16}O$ isotopologue were measured with a typical accuracy of 5.0×10^{-4} cm^{-1}. The transitions were rovibrationally assigned on the basis of the global effective Hamiltonian model. The band by band analysis allowed for the determination of the rovibrational parameters of a total of 73 bands. 29 of them are newly reported and more rotational transitions have been observed for the others. The maximum deviation of the preidictions of the effective Hamiltonian model is up to 0.70 cm^{-1} for the $^{15}N_2^{16}O$ species.

Key words: Infrared spectroscopy, $^{15}N_2^{16}O$, High-resolution, Effective Hamiltonian

I. INTRODUCTION

As an important atmospheric trace gas, nitrous oxide is involved in greenhouse effect and stratospheric ozone depletion. In particular, the stable nitrogen compositions of N_2O ($\delta^{15}N$) can provide an invaluable insight into understanding its atmospheric sources and sinks. In the past decade, the advances in laser technology and CRDS technique open up the tendency of new method in monitoring the concentration of the extremely low level atmospheric tracer, compared with mass spectroscopy. It needs a comprehensive knowledge of different isotopologues spectrum in the infrared region. The present contribution is the continuation of a series devoted to the systematic study of the infrared absorption spectrum of nitrous oxide isotopologues from middle to near infrared region [1−5]. The line position and intensity parameters of the $^{15}N_2^{16}O$ isotopologue have also been studied by Amiot [6], Toth [7], and Lyulin *et al.* [8] in the 1750−6000 and 5800−7600 cm^{-1} region, respectively. The information obtained in present work together with previous studies will help to make the new global fitting of effective Hamiltonian and dipole parameters for the $^{15}N_2^{16}O$ isotopologue as the main isotopologue $^{14}N_2^{16}O$ [9, 10] and other two isotopologues $^{14}N^{15}N^{16}O$ and $^{15}N^{14}N^{16}O$ [11].

In this work, 7343 transitions of 73 bands have been studied between 1650 and 3450 cm^{-1} for the $^{15}N_2^{16}O$ isotopologue. The vibrational assignments and a band-by-band rotational analysis are presented.

II. EXPERIMENTS

The $^{15}N_2^{16}O$ enriched nitrous oxide sample was purchased from Icon Services Inc with stated purity of 98%. The absorption spectrum in 1650−3450 cm^{-1} region was recorded by a Bruker IFS 120HR interferometer equipped with a multi-pass gas cell with an adjustable path length. The whole interference chamber was evacuated to less than 40 Pa to reduce background absorption and interference from atmospheric gases. Because of the wide spectral range and the large variations in absorption band intensities, different experimental conditions were applied for the measurements, as listed in Table I. The gas sample pressure was measured using the manometers (MKS Baratron 627B) with 2.6 kPa full-scale range and 0.15% accuracy. Different optical filters were applied to improve the signal-to-noise ratio and to allow the high-resolution measurements. The line positions were calibrated using the absorption lines of water and carbon dioxide. Their values were taken from the Hitran2008 database [12]. The accuracy of the unblended and not-very-weak lines is estimated to be better than 5×10^{-4} cm^{-1}. Overview spectrum of $^{15}N_2^{16}O$ enriched sample in the whole studied region is presented in Fig.1.

TABLE I Experimental conditions of $^{15}N_2^{16}O$ enriched nitrous oxide sample including wavenumber ranger, pressure p, path length L, resolution R, and temperature T.

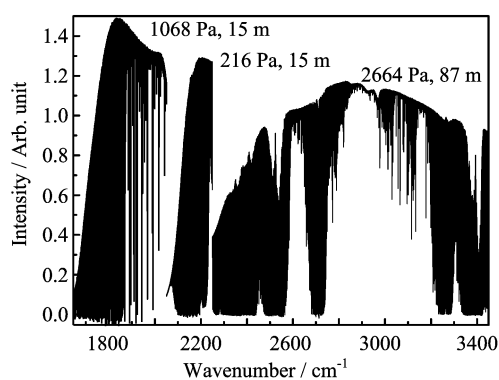| Range/cm^{-1}	p/Pa	Source	L/m	R/10^{-3}cm^{-1}	T/K
1700−2100	216	Globar	15	6	294
1700−2100	1068	Globar	15	6	293
2000−2400	216	Tungsten	15	4	297
2000−2400	1068	Tungsten	15	4	291
2000−2400	2664	Tungsten	15	4	292
2550−3250	216	Tungsten	15	5	293
2550−3250	1068	Tungsten	15	5	291
2550−3250	2664	Tungsten	15	5	293
2550−3250	1515	Tungsten	87	5	292
1800−8500	2664	Tungsten	87	1.5	292

FIG. 1 The Fourier-transform absorption spectrum of $^{15}N_2^{16}O$ enriched sample in the 1650−3450 cm^{-1} region.

III. ROVIBRATIONAL ANALYSIS

A. Vibrational assignment

Total 7343 transitions were assigned based on the predictions of the effective Hamiltonian of Ref.[8]. The adopted effective Hamiltonian is based on a polyad structure resulting from the approximate relations between the harmonic frequencies $\omega_3 \approx 2\omega_1 \approx 4\omega_2$. Since the mix between the $(v_1, v_2 l_2, v_3)$ states may be strong, the vibrational energy levels are labeled using the triplet $(P=2v_1+v_2+4v_3, l_2, i)$, where the index i increases with energy.

All absorptions in the studied region corresponds to $\Delta P < 7$. Among the 73 $^{15}N_2^{16}O$ bands which were identified, there are 45 parallel ($\Delta l_2=0$) bands (23 Σ-Σ, 11 Π-Π, 8 Δ-Δ, 2 Φ-Φ, 1 Γ-Γ), 25 perpendicular ($\Delta l_2=1$) bands (11 Π-Σ, 7 Σ-Π, 3 Π-Δ, 2 Δ-Π, 2 Φ-Δ), and 3 Δ-Σ cold ($\Delta l_2=2$) bands. Figure 2 shows the Q-branch of (2110)←(0000) Π-Σ cold band centered at 3102.82 cm^{-1}.

TABLE II Lower states constants of the rovibrational bands of $^{15}N^{15}N^{16}O$ assigned in the FTS spectra.

$v_1v_2l_2v_3$	G_v	$B_v \times 10^3$	$D_v \times 10^7$	$H_v \times 10^9$
0000e[a]	0.0	404.8602	1.635600	
0110e[a]	571.89400	405.0021	1.656000	
0110f[a]	571.89400	405.7617	1.663800	
0200e[a]	1136.45300	405.7410	2.294000	
0220e[b]	1143.961	405.913	1.112	
0220f[b]	1143.961	405.9	1.698	
1000e[a]	1265.33383	403.153720	1.627990	
0310e[b]	1701.9954	405.438	1.987	
0310f[b]	1701.9954	406.897	2.046	
0330e[a]	1716.1856	406.393	1.387	
1110e[a]	1842.40670	403.3186	1.637500	
1110f[a]	1842.40670	404.1670	1.620000	
0001e[a]	2154.72590	401.61709	1.627970	−87.000

[a] The lower state constants were fixed at the values of Ref.[7].
[b] The lower state constants were fixed at the values of Ref.[6].

B. Band by band rotational analysis

In the case of unperturbed bands, the rotational analysis was performed using the standard equation for the vibration-rotation energy levels:

$$F_v(J) = G_v + B_v J(J+1) - D_v J^2 (J+1)^2 + H_v J^3 (J+1)^3 \tag{1}$$

where G_v is the vibrational term value, B_v is the rotational constant, D_v and H_v are centrifugal distortion constants. The spectroscopic parameters for an upper state were fitted directly to the observed line positions of the respective band, and in the case of hot bands involving e and f rotational levels, the ee, ef, fe and ff sub bands were considered independently. The lower state rotational constants were constrained to their literature values [6, 7]. The global line list provided as Supplementary Material includes the deviations between the measured values and the values calculated with the fitted rovibrational parameters.

The spectroscopic parameters retrieved from the fit of the line positions are listed in Tables II−IV for cold and hot bands, respectively. For 44 previous reported bands, our work looked at transitions of higher J values and gave more accurate spectroscopic constants than Amiot's work [6], which are reviewed and given in Tables II−IV. The rms values of the (obs.−calc.) deviations are generally smaller than 10^{-3} cm^{-1} which is consistent with the experimental uncertainty on the line positions. It is worth noting that the lower state rotational constants of two bands rising from (0400) and (0420) lower vibrational states were constrained to the values newly determined in this work. As indi-

TABLE III Spectroscopic parameters (in cm^{-1}) of the rovibrational bands of $^{15}N^{15}N^{16}O$ assigned in the FTS spectra between 1650 and 3450 cm^{-1}. The cold and hot bands are listed successively and ordered according to their ΔG_v values, which is the difference between the upper and lower vibrational term values. The uncertainties are given in parenthesis in the unit of the last quoted digit. When a given band has been previously analyzed, the corresponding spectroscopic parameters are given in italics for comparison.

ΔG_v	Type	Bands[a]	(P, l_2, i)[b]	G_v	$B_v \times 10^3$	$D_v \times 10^7$	$H_v \times 10^{12}$
				Cold bands			
1701.994395(72)	Π-Σ	0310e-0000e	(3 1 1)	1701.994395(72)	405.43590(22)	1.9646(13)	
1701.993921(63)		0310f-0000e		1701.993921(63)	406.90120(18)	2.07912(88)	
1842.406817(32)	Π-Σ	1110e-0000e	(3 1 2)	1842.406817(32)	403.318171(45)	1.63601(12)	
1842.4069(2)[c]		*1110e-0000e*			*403.3186(1)*	*1.6375(2)*	
1842.40710(13)		1110f-0000e		1842.40710(13)	404.30720(15)	1.63607(34)	
1842.4069(2)		*1110f-0000e*			*404.167(2)*	*1.620(2)*	
2154.73048(69)	Σ-Σ	0001e-0000e	(4 0 1)	2154.73048(69)	401.61558(20)	1.62868(13)	
2154.7256(1)[c]		*0001e-0000e*			*401.61732(4)*	*1.6301(1)*	
2261.469245(64)	Σ-Σ	0400e-0000e	(4 0 2)	2261.469245(64)	406.48787(25)	4.2223(22)	21.023(51)
2261.4695(1)[c]		*0400e-0000e*			*406.4882(3)*	*4.227(3)*	
2268.30589(28)	Δ-Σ	0420e-0000e	(4 2 1)	2268.30589(28)	406.58531(75)	$-0.3829(56)$	$-21.05(13)$
2409.45644(16)	Σ-Σ	1200e-0000e	(4 0 3)	2409.45644(16)	404.07391(24)	2.4171(12)	3.464(17)
2409.4564(1)[c]		*1200e-0000e*			*404.0737(1)*	2.4148(5)	*3.42(6)*
2418.15162(94)	Δ-Σ	1220e-0000e	(4 2 2)	2418.15162(94)	404.3157(16)	1.0012(73)	$-2.990(97)$
2418.9466(1)[c]		*1220e-0000e*			*404.2965(1)*	*0.9386(5)*	$-3.59(7)$
2523.2793(15)	Σ-Σ	2000e-0000e	(4 0 4)	2523.2793(15)	401.46924(67)	1.54465(74)	
2523.2538(1)[c]		*2000e-0000e*			*401.4876(1)*	*1.5871(4)*	*3.23(6)*
2713.143232(38)	Π-Σ	0111e-0000e	(5 1 1)	2713.143232(38)	401.800123(32)	1.648359(56)	
2713.1440(1)[c]		*0111e-0000e*			*401.80017(2)*	*1.64830(5)*	
2713.14324(21)		0111f-0000e		2713.14324(21)	402.68760(19)	1.67955(39)	
2713.1440(1)		*0111f-0000e*			*402.687(1)*	*1.680(2)*	
2822.13432(11)	Π-Σ	0510e-0000e	(5 1 2)	2822.13432(11)	405.75049(51)	2.4632(44)	
2977.73656(11)	Π-Σ	1310e-0000e	(5 1 3)	2977.73656(11)	403.69378(38)	1.9949(30)	1.500(63)
2977.74387(20)		1310f-0000e		2977.74387(20)	405.28930(36)	2.1591(12)	1.593(90)
3105.938221(64)	Π-Σ	2110e-0000e	(5 1 4)	3105.938221(64)	401.67900(12)	1.59746(33)	
3105.9393(2)[c]		*2110e-0000e*			*401.64(2)*	*2.26(36)*	
3105.938042(78)		2110f-0000e		3105.938221(64)	402.78800(22)	1.5612(11)	
3105.9393(2)		*2110f-0000e*			*402.646(3)*	*1.540(2)*	
3264.708885(72)	Σ-Σ	0201e-0000e	(6 0 1)	3264.708885(72)	402.59170(19)	2.4872(12)	4.394(21)
3264.7111(1)[c]		*0201e-0000e*			*402.5920(1)*	*2.489(1)*	*4.45(2)*
3271.8192(11)	Δ-Σ	0221e-0000e	(6 2 1)	3271.8192(11)	402.7434(17)	1.0876(58)	
				Hot bands			
1689.59070(44)	Σ-Π	0400e-0110f	(4 0 2)	2261.48470(44)	406.6408(53)	6.83(16)	1.55(15)
1696.41142(35)	Δ-Δ	0420e-0110f		2268.30542(35)	406.5953(18)	$-0.084(18)$	
1696.41100(39)		0420f-0110e		2268.30500(39)	406.5940(25)	2.061(29)	
1833.77743(17)	Π-Δ	1310e-0220e	(5 1 3)	2977.73843(17)	403.7082(10)	2.087(11)	
1833.77663(17)		1310f-0220f		2977.73763(17)	405.27083(60)	2.0608(42)	
1837.562277(49)	Σ-Π	1200e-0110e	(4 0 3)	2409.456277(49)	404.07427(20)	2.4143(19)	3.341(48)
1837.5627(5)[c]		*1200e-0110e*			*404.0735(3)*	*2.396(7)*	*2.3(4)*
1837.56296(18)		1200e-0110f		2409.45696(18)	404.06630(53)	2.3157(28)	
1837.5627(5)		*1200e-0110f*			*404.073(1)*	*2.416(16)*	*3.5(9)*
1840.603823(87)	Π-Σ	2110e-1000e	(5 1 4)	3105.937653(87)	401.68088(26)	1.6076(14)	
1840.604498(23)		2110f-1000e		3105.938328(23)	402.6449(10)	1.5250(86)	
1841.28493(11)	Π-Σ	1310e-0200e	(5 1 3)	2977.73793(11)	403.67581(34)	1.8760(18)	
1841.28481(20)		1310f-0200e		2977.73781(20)	405.24730(81)	1.9412(61)	

To be continued.

Table III continued.

ΔG_v	Type	Bands[a]	(P, l_2, i)[b]	G_v	$B_v \times 10^3$	$D_v \times 10^7$	$H_v \times 10^{12}$
				Hot band			
1847.052081(63)	Δ-Π	1220e-0110e	(4 2 2)	2418.946081(63)	404.29807(25)	0.9483(22)	−3.410(54)
1847.0524(1)[c]		*1220e-0110e*			*404.2986(3)*	*0.957(6)*	*−3.0(3)*
1847.052179(38)		1220f-0110f		2418.946179(38)	404.297322(74)	1.642374(26)	
1847.0524(1)		*1220f-0110f*			*404.2977(2)*	*1.644(1)*	
1847.05136(18)		1220e-0110f		2418.94536(18)	404.30300(53)	1.0380(29)	
1847.0524(1)		*1220e-0110f*			*404.297(1)*	*0.953(5)*	*−3.1(3)*
1847.05211(13)		1220f-0110e		2418.94611(13)	404.29880(29)	1.6449(12)	
1851.09799(11)	Φ-Δ	1330e-0220e	(5 3 2)	2995.05899(11)	404.8403(38)	0.8530(21)	
1851.097(1)[c]		*1330e-0220e*			*404.73(3)*	*1.422(35)*	
1951.359778(60)	Σ-Π	2000e-0110e	(4 0 4)	2523.253778(60)	401.48630(11)	1.57251(36)	
1951.3600(1)[c]		*2000e-0110e*			*401.48737(7)*	*1.5785(5)*	
1951.35912990(87)		2000e-0110f		2523.25312990(87)	401.4897807(23)	1.596728(11)	
1951.3600(1)		*2000e-0110f*			*401.486(1)*	*1.575(1)*	
1961.97804(12)	Π-Δ	2110e-0220e	(5 1 4)	3105.93904(12)	401.69406(43)	1.6989(29)	
1961.977398(73)		2110f-0220f		3105.938398(73)	402.65149(23)	1.5519(14)	
1961.97727(18)		2110e-0220f		3105.93827(18)	401.68520(65)	1.6135(46)	
1961.97816(19)		2110f-0220e		3105.93916(19)	402.66049(80)	1.6393(60)	
1969.45565(10)	Π-Σ	2110e-0200e	(5 1 4)	3105.93865(10)	401.66269(38)	1.5062(26)	
2101.615464(94)	Γ-Γ	0441e-0440e	(8 4 1)	−[d]	404.0679(22)	2.308(11)	
2101.97804(18)	Π-Π	1221e-1220e	(8 2 3)	4520.92412(18)	401.12971(70)	1.0171(48)	
2101.97828(17)		1221f-1220f		4520.92446(17)	401.12422(69)	1.6265(48)	
2102.35030(20)	Σ-Σ	2001e-2000e[e]	(8 0 5)	4625.60370(20)	398.22311(89)	1.5839(76)	
2102.37982(17)	Δ-Δ	0421e-0420e	(8 2 1)	4370.68524(17)	403.49424(40)	−0.1441(17)	
2102.37892(15)		0421f-0420f		4370.68392(15)	403.49769(39)	2.0580(19)	
2102.424019(99)	Σ-Σ	1201e-1200e	(8 0 4)	4511.880459(99)	400.89811(42)	2.3305(33)	
2102.72159(24)	Σ-Σ	0401e-0400e[e]	(8 0 2)	4364.19083(24)	403.3779(11)	3.890(10)	
2114.581738(88)	Φ-Φ	0331e-0330e	(7 3 1)	3830.767338(88)	403.25625(10)	1.36926(21)	
2114.5819(1)[c]		*0331e-0330e*			*403.258(4)*	*1.37(4)*	
2115.292245(58)	Π-Π	0311e-0310e	(7 1 1)	3817.287645(58)	402.318947(71)	1.98365(15)	
2115.2924(1)[c]		*0311e-0310e*			*402.320(5)*	*1.985(43)*	
2115.292355(68)		0311f-0310f		3817.287755(68)	403.746540(72)	2.03954(13)	
2115.2924(1)		*0311f-0310f*			*403.747(3)*	*2.04(3)*	
2115.335118(95)[d]	Π-Π	1111e-1110e	(7 1 3)	3957.741818(95)	400.11534(14)	1.62523(37)	
2115.3351(2)[c]		*1111e-1110e*			*400.116(2)*	*1.639(21)*	
2115.335056(79)		1111f-1110f		3957.741756(79)	400.94057(16)	1.61089(56)	
2115.3351(2)		*1111f-1110f*			*400.943(2)*	*1.636(15)*	
2126.614351(51)	Σ-Σ	0002e-0001e[e]	(8 0 1)	4281.340251(51)	398.367460(77)	1.62269(20)	
2127.86936(36)	Δ-Δ	0221f-0220f	(6 2 1)	3271.83036(36)	402.72603(18)	1.69106(19)	
2127.8688(1)[c]		*0221f-0220f*			*402.747(3)*	*1.744(9)*	
2128.25829(51)	Σ-Σ	0201e-0200e	(6 0 1)	3264.71129(51)	4026965(24)	2.29620(25)	
2128.2569(1)[c]		*0201e-0200e*			*402.592(1)*	*2.483(7)*	*4.3(1)*
2128.83097(66)	Σ-Σ	1001e-1000e	(6 0 3)	3394.16480(66)	399.89907(34)	1.62026(40)	
2128.8285(1)[c]		*1001e-1000e*			*399.8996(1)*	*1.6101(6)*	
2141.25050(63)	Π-Π	0111e-0110e	(5 1 2)	2713.14450(63)	401.80021(22)	1.64837(19)	
2141.2506(1)[c]		*0111e-0110e*			*401.80039(4)*	*1.6486(1)*	
2141.25063(63)		0111f-0110f		2713.14463(63)	402.54464(22)	1.65800(18)	
2141.2506(1)		*0111f-0110f*			*402.54491(4)*	*1.6583(8)*	
2239.83651(16)	Δ-Δ	0620e-0220e	(6 2 2)	3383.79751(16)	407.2075(12)	−1.749(18)	
2239.836(2)[c]		*0620e-0220e*			*407.192(14)*	*−1.79(12)*	

To be continued.

Table III continued.

ΔG_v	Type	Bands[a]	(P, l_2, i)[b]	G_v	$B_v \times 10^3$	$D_v \times 10^7$	$H_v \times 10^{12}$
2239.83737(11)		0620f-0220f		3383.79837(11)	407.18598(65)	2.5233(72)	
2239.836(2)		*0620f-0220f*			*407.181(7)*	*2.510(54)*	
2240.98319(16)	Σ-Σ	0600e-0200e	(6 0 2)	3377.43619(16)	407.0716(17)	6.578(42)	43.9 (29)
2240.9833(1)[c]		*0600e-0200e*			*407.098(5)*	*6.89(12)*	*5.56(93)*
2250.241650(76)	Π-Π	0510e-0110e	(5 1 2)	2822.135650(76)	405.75409(34)	2.5569(34)	5.908 (94)
2250.2416(1)[c]		*0510e-0110e*			*405.7539(4)*	*2.552(5)*	*5.7(1)*
2250.241352(35)		0510f-0110f		2822.135352(35)	407.89491(17)	2.6845(20)	−3.365(59)
2250.2416(1)		*0510f-0110f*			*407.8952(3)*	*2.688(4)*	*−3.2(1)*
2402.02866(13)	Σ-Σ	1400e-0200e[f]	(6 0 4)	3538.48166(13)	404.72825(68)	3.8726(83)	12.38(26)
2402.0289(1)[c]		*1400e-0200e*			*404.756(4)*	*4.128(40)*	*1.91(11)*
2402.76036(23)	Δ-Δ	1420e-0220e	(6 2 3)	3546.72136(23)	404.9727(54)	5.39(27)	874(36)
2402.7607(7)[c]		*1420e-0220e*			*404.906(17)*	*1.07(27)*	
2402.76114(11)		1420f-0220f		346.72214(11)	404.92348(64)	2.3202(18)	
2402.7607(7)		*1420f-0220f*			*404.919(9)*	*2.30(28)*	
2405.844547(49)	Π-Π	1310e-0110e	(5 1 3)	2977.738547(49)	403.69326(17)	1.9885(13)	1.376(28)
2405.8446(1)[c]		*1310e-0110e*			*403.6929(1)*	*1.9853(7)*	*1.30(1)*
2405.844246(53)		1310f-0110f		2977.738246(53)	405.264424(94)	2.04278(30)	
2405.8446(1)		*1310f-0110f*			*402.6352(7)*	*2.0340(5)*	*−0.19(1)*
2409.378564(92)	Σ-Σ	2200e-1000e[f]	(6 0 4)	3674.712394(92)	402.37290(36)	2.2950(26)	
2409.3785(1)[c]		*2200e-1000e*			*402.374(1)*	*2.329(16)*	*2.0(6)*
2508.902173(76)	Σ-Σ	3000e-1000e[f]	(6 0 6)	3774.236003(76)	399.90874 (21)	1.47959(95)	
2508.9030(1)[c]		*3000e-1000e*			*399.9095(1)*	*1.492(1)*	*0.64(4)*
2520.55498(19)	Π-Π	3110e-1110e[f]	(7 1 6)	4362.96168(19)	400.1115 (10)	1.5482(90)	
2520.556(2)[c]		*3110e-1110e*			*400.109(1)*	*1.515(10)*	
2520.55551(27)		3110f-1110f		4362.96221(27)	401.2419(11)	1.4139(93)	
2520.556(2)		*3110f-1110f*			*401.239(3)*	*1.393(23)*	
2534.04533(18)	Π-Π	2110e-0110e	(5 1 4)	3105.93933(18)	401.67790(11)	1.59352(16)	
2534.0453(1)[c]		*2110e-0110e*			*401.68020(4)*	*1.6060(4)*	*0.180(5)*
2534.04865(25)		2110f-0110f		3105.94265(25)	402.63946(22)	1.52035(47)	
2534.0453(1)		*2110f-0110f*			*402.64574(8)*	*1.5479(5)*	*0.377(7)*
2538.259591(96)	Σ-Σ	2200e-0200e	(6 0 5)	3674.712591(96)	402.35511(36)	2.1984(25)	
2538.2607(1)[c]		*2200e-0200e*			*402.373(1)*	*2.340(9)*	*2.7(1)*
2543.13468(11)	Δ-Δ	2220e-0220e	(6 2 4)	3687.09568(11)	4028273(42)	1.1326(27)	
2543.1355(1)[c]		*2220e-0220e*			*402.758(4)*	*0.913(22)*	*−4.0(4)*
2543.134636(98)		2220f-0220f		3687.095636(98)	402.76916(39)	1.5901(24)	
2543.1355(1)		*2220f-0220f*			*402.762(2)*	*1.573(5)*	
2543.62078(27)	Π-Π	2310e-0310e[e]	(7 1 6)	4245.61618(27)	401.9407(14)	2.044(12)	
2543.6223(1)[c]		*2310e-0310e*			*401.932(2)*	*1.933(14)*	
2543.62197(22)		2310f-0310f		4245.61737(22)	403.6276(12)	1.952(12)	
2543.6223(1)		*2310f-0310f*			*403.631(3)*	*1.977(18)*	
2550.89476(14)	Φ-Φ	2330e-0330e	(7 3 3)	4267.08036(14)	403.31398(49)	1.3506(32)	
2550.8958(5)[c]		*2330e-0330e*			*403.307(7)*	*1.344(36)*	
2637.78411(16)	Σ-Σ	3000e-0200e	(6 0 6)	3774.23711(16)	399.88958(72)	1.3711(60)	
2673.32523(19)	Π-Δ	0311e-0220e	(7 1 1)	3817.28623(19)	402.3386(15)	2.112(12)	
2673.32526(16)		0311f-0220f		3817.28626(16)	403.75601(44)	2.0823(23)	
2680.83398(13)	Π-Σ	0311e-0200e	(7 1 1)	3817.28698(15)	402.2993(13)	1.852(21)	
2680.8348(1)[c]		*0311e-0200e*			*402.317(3)*	*1.960(10)*	*3.3(16)*
2686.80601(12)	Φ-Δ	0331e-0220e	(7 3 1)	3830.76701(12)	403.27819(61)	1.5725 (61)	
2686.8065(5)[c]		*0331e-0220e*			*403.260(4)*	*1.461(24)*	
2686.80545(12)		0331f-0220f		3830.76645(12)	403.26559(69)	1.4198(67)	

To be continued.

Table III continued.

ΔG_v	Type	Bands[a]	(P, l_2, i)[b]	G_v	$B_v \times 10^3$	$D_v \times 10^7$	$H_v \times 10^{12}$
2686.8065(5)		*0331f-0220f*			*403.263(4)*	*1.429(20)*	
2692.40656(12)	Π-Σ	1111e-1000e	(7 1 3)	3957.74039(12)	400.11737(30)	1.6358(13)	
2692.40721(26)		1111f-1000e		3957.77410(26)	400.94260(81)	1.6280(45)	
2692.814711(44)	Σ-Π	0201e-0110e	(6 0 1)	3264.708711 (44)	402.59200(12)	2.48473(78)	4.327(13)
2692.8156(3)[c]		*0201e-0110e*			*402.5923(1)*	2.4876(9)	4.38(2)
2692.81552(17)		0201e-0110f		3264.70952(17)	402.58320(54)	2.3683(31)	
2692.8156(3)		*0201e-0110*f			*402.590(2)*	*2.474(6)*	*4.0(3)*
2699.935440(61)	Δ-Π	0221e-0110e	(6 2 1)	3271.829440(61)	402.71973(19)	0.9051(14)	−4.339(27)
2699.9362(3)[c]		*0221e-0110e*			*402.7196(2)*	0.906(2)	−4.25(6)
2699.935356(77)		0221f-0110f		3271.829356(77)	402.71989(17)	1.67670(66)	
2699.9362(3)		*0221f-0110f*			*402.7199(1)*	*1.6764(4)*	
2699.93494(12)		0221f-0110e		3271.82894(12)	402.72150(25)	1.67923(93)	
2699.9362(3)		*0221f-0110e*			*402.722(2)*	*1.679(2)*	
2699.93453(19)		0221e-0110f		3271.82853(19)	402.72630(57)	1.0205(31)	
2699.9362(3)		*0221e-0110f*			*402.718(1)*	*0.909(10)*	*−4.0(3)*
2822.268568(52)	Σ-Π	1001e-0110e	(6 0 3)	3394.162568(52)	399.8993(64)	1.614214(93)	
2822.2695(2)[c]		*1001e-0110e*			*399.8988(4)*	*1.608(4)*	
2822.268531(78)		1001e-0110f		3394.162531(78)	399.89780(20)	1.60897(86)	
2822.2695(2)		*1001e-0110f*			*399.8987(4)*	*1.612(3)*	
2966.58698(23)	Σ-Π	1400e-0110e	(6 0 4)	3538.48098(23)	404.7412(16)	3.816(19)	
2966.58981(41)		1400e-0110f		3538.48381(41)	404.7316(20)	3.732(17)	
3016.005788(34)	Σ-Σ	0002e-1000e[f]	(8 0 1)	4281.339618(56)	398.36905(14)	1.63426(66)	
3102.81689(32)	Σ-Π	2200e-0110e	(6 0 5)	3674.71089(32)	40.23841(14)	2.454(17)	6.26(56)
3102.81891(31)		2200e-0110f		3674.71291(31)	402.3730(16)	2.315(15)	
3144.88881(23)	Σ-Σ	0002e-0200e	(8 0 1)	4281.34181(23)	398.3448(14)	1.428(20)	−4.81(74)
3226.72375(15)	Δ-Δ	0421e-0220e	(8 2 1)	4370.68475(15)	403.51001(60)	−0.2027(59)	−17.59(15)
3226.72415(13)		0421f-0220f		4370.68515(13)	403.49903(44)	2.0512(36)	0.742(81)
3227.73725(15)	Σ-Σ	0401e-0200e	(8 0 2)	4364.19025(15)	403.36856(58)	4.0206(52)	17.00(12)
3245.392955(86)	Π-Π	0311e-0110e	(7 1 1)	3817.286955(86)	402.31942(28)	1.9965(21)	1.556(42)
3245.3949(1)[c]		*0311e-0110e*			*402.3192(4)*	*1.995(6)*	*1.4(2)*
3245.392433(76)		0311f-0110f		3817.286433(76)	403.75176(14)	2.08263(47)	
3245.3949(1)		*0311f-0110f*			*403.7498(1)*	*2.069(1)*	
3246.54465(23)	Σ-Σ	1201e-1000e[f]	(8 0 4)	4511.57848(23)	400.9028(12)	2.359(15)	
3360.26959(15)	Σ-Σ	2001e-1000e[e]	(8 0 5)	4625.60342(15)	398.22321(54)	1.5744(37)	
3360.2717(1)[c]		*2001e-1000e*			*398.2227(1)*	*1.5687(9)*	
3375.42732(17)	Σ-Σ	1201e-0200e	(8 0 4)	4511.88032(17)	400.87975(66)	2.2156(45)	
3375.4294(2)[c]		*1201e-0200e*			*400.897(2)*	*2.313(7)*	
3376.96231(39)	Δ-Δ	1221e-0220e	(8 2 3)	4520.92331(39)	401.1589(71)	1.54(25)	
3376.9658(2)[c]		*1221e-0220e*			*401.106(3)*	*0.903(12)*	
3385.84892(23)[e]	Π-Π	1111e-0110e	(7 1 3)	3957.74292(23)	400.11548(40)	1.6258(15)	
3385.8533(3)[c]		*1111e-0110e*			*400.1191(7)*	*1.661(6)*	*0.8(1)*
3385.84606(11)		1111f-0110f		3957.74006(17)	400.94040(34)	1.6100(13)	
3385.8533(3)		*1111f-0110f*			*400.9363(5)*	*1.602(1)*	

[a] Normal mode labeling according to the maximum value of the modulo of the expansion coefficients of an eigenfunction. In the cases when there are two candidates for the same labeling or modulo of two principal expansion coefficients practically coincide, we give in parentheses the second variant of the labeling. Note that as a result of strong vibrational mixing, the normal mode labeling of some states differs from that given in the previous analysis.
[b] Cluster labelling notation: ($P=2v_1+v_2+4v_3$, l_2, i) for the upper state of the band, i is the order number within the cluster increasing with the energy.
[c] Ref.[6].
[d] The vibrational term values are not given due to the absence of the vibrational term value of the lower vibrational state.
[e] The previous work can be find in Ref.[4].
[f] The previous work can be find in Refs.[4, 6].

©2011 Chinese Physical Society

TABLE IV Other spectroscopic parameters of the cold bands of $^{15}N^{15}N^{16}O$ assigned in the FTS spectra.

ΔG_v	Observed lines	n/N^a	RMS$\times10^3$
1701.994395(72)	P42/R43	82/84	0.32
1701.993921(63)	Q66	49/49	0.38
1842.406817(32)	P66/R64	129/129	0.19
1842.40710(13)	Q47	46/47	0.22
2154.73048(69)	P100/R89	43/47	0.16
2261.469245(64)	P56/R53	107/109	0.29
2268.30589(28)	P54/R50	60/62	0.31
2409.45644(16)	P70/R58	48/48	0.22
2418.15162(94)	P48/R67	29/34	0.85
2523.2793(15)	P67/R77	29/33	0.25
2713.143232(38)	P78/R78	127/128	0.19
2713.14324(21)	Q67	37/37	0.40
2822.13432(11)	P25/R40	48/59	0.35
2977.73656(11)	P37/R58	88/94	0.46
2977.74387(20)	Q55	46/50	0.56
3105.938221(64)	P21/R62	80/82	0.37
3105.938042(78)	Q46	46/46	0.27
3264.708885(72)	P66/R53	104/106	0.32
3271.8192(11)	P49/R40	33/39	0.63

[a] n: number of transitions included in the fit, N: number of assigned rotational transitions.

FIG. 3 Overview of the calculated transitions of $^{15}N_2^{16}O$. The transitions which were assigned in present FTS study are highlighted (circle in red). Line positions were calculated with the effective Hamiltonian parameters of Ref.[9]. Line intensities are approximate values obtained with the effective dipolar momentum of Ref.[10]. A logarithmic scale is used for the line intensities. For the interpretation of the color in this figure legend, the reader can refer to the web version of this article.

FIG. 4 Difference between the line positions of the $^{15}N_2^{16}O$ isotopologues of nitrous oxide assigned in the FTS spectrum in present study and their values predicted by the effective rovibrational Hamiltonian [9].
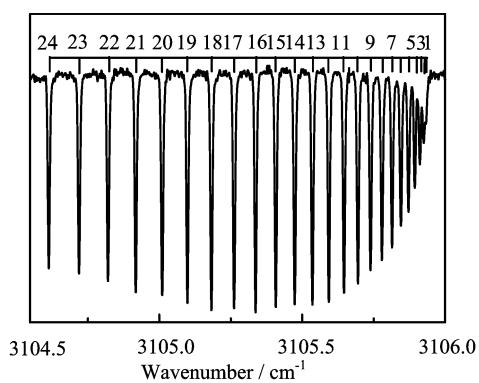

FIG. 2 The Q branch of the (2110)←(0000) Π-Σ cold band of $^{15}N_2^{16}O$ at 3102.82 cm^{-1} and the rotational assignments are presented. The spectrum was recorded at a pressure of 2664 Pa and equivalent path length of 15 m.

cated in Table III−IV, only the difference between the upper and lower vibrational term values, the B_v and D_v values of lower and upper vibrational states of the (0441)←(0440) Γ-Γ band were determined, due to the absence of the spectroscopic constants of (0440) lower state with very high angular quantum number. The transitions assigned to $^{15}N_2^{16}O$ are highlighted on Fig.3 which presents the overview spectrum as predicted by the polyad model [9, 10]. Due to no input experimental intensity information, the set of the effective dipole mo-
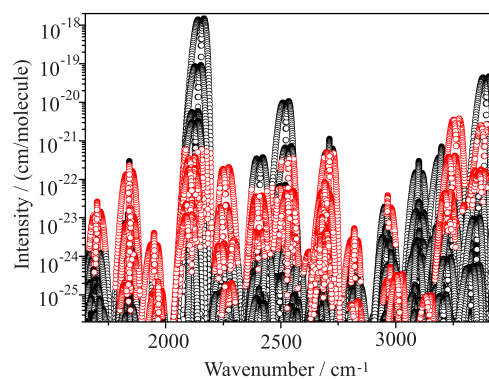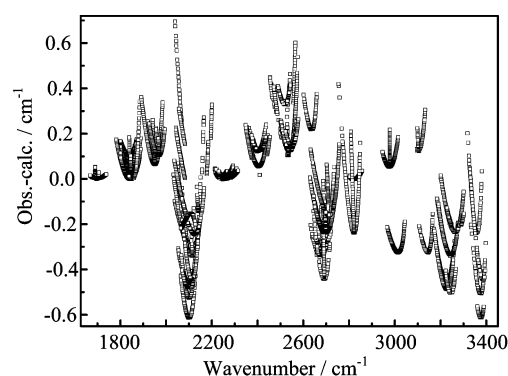
mentum of the $^{14}N_2^{16}O$ isotopologue [10] was used for $^{15}N_2^{16}O$ in the calculation. The sensitivity in this work is about 5×10^{-25} cm/molecule in 1650−2100 cm^{-1} and 10^{-25} cm/molecule in 2100−3450 cm^{-1}. Our observations show some important deviations between the calculated intensities and our measurements. For instance, some bands predicted with intensity much above our detection sensitivity threshold have not been detected, indicating that the corresponding predicted intensities are overestimated, while some other bands are obviously underestimated.

IV. DISCUSSION AND CONCLUSION

The differences between the measured line positions of the $^{15}N_2^{16}O$ isotopologue and their predicted val-

TABLE V Spectroscopic parameters (in cm^{-1}) of the hot bands of ^{15}N^{15}N^{16}O assigned in the FTS spectra

ΔG_v	Observed lines	n/N	RMS$\times 10^3$	ΔG_v	Observed lines	n/N	RMS$\times 10^3$
1689.59070(44)	Q29	27/28	0.82	2402.02866(13)	P45/R47	58/69	0.41
1696.41142(35)	Q33	29/30	0.82	2402.76036(23)	P23/R21	22/22	0.37
1696.41100(39)	Q29	24/25	0.84	2402.76114(11)	P59/R57	31/34	0.36
1833.77743(17)	P32/R20	27/32	0.38	2405.844547(49)	P60/R49	101/104	0.21
1833.77663(17)	P39/R22	36/36	0.38	2405.844246(53)	P62/R50	105/108	0.28
1837.5627(5)	P51/R52	96/101	0.21	2409.378564(92)	P42/R34	54/65	0.36
1837.56296(18)	Q46	45/46	0.64	2508.902173(76)	P54/R52	40/48	0.29
1840.603823(87)	P45/R42	74/82	0.35	2520.55498(19)	P34/R32	26/32	0.42
1840.604498(23)	Q35	27/29	0.60	2520.55551(27)	P33/R31	28/32	0.44
1841.28493(11)	P45/R42	68/85	0.46	2534.04533(18)	P61/R88	51/51	0.46
1841.28481(20)	Q37	24/28	0.43	2534.04865(25)	P63/R63	60/66	0.34
1847.052081(63)	P55/R47	96/98	0.25	2538.259591(96)	P40/R38	63/70	0.37
1847.052179(38)	P51/R56	97/102	0.20	2543.13468(11)	P43/R41	50/70	0.43
1847.05136(18)	Q50	40/45	0.52	2543.134636(98)	P42/R40	45/54	0.37
1847.05211(13)	Q51	45/48	0.43	2543.62078(27)	P34/R32	19/35	0.52
1851.09799(11)	P15/R43	42/48	0.39	2543.62197(22)	P29/R30	20/24	0.42
1951.359778(60)	P62/R54	110/116	0.32	2550.89476(14)	P31/R39	41/46	0.40
1951.35912990(87)	Q47	47/47	0.00	2637.78411(16)	P36/R34	56/56	0.51
1961.97804(12)	P44/R33	63/71	0.45	2673.32526(19)	P36/R34	26/28	0.49
1961.977398(73)	P45/R36	67/74	0.29	2673.32526(16)	P45/R43	34/38	0.41
1961.97727(18)	Q38	30/32	0.40	2680.83398(13)	P25/R23	37/44	0.37
1961.97816(19)	Q37	33/33	0.54	2686.80601(12)	P33/R31	46/58	0.35
1969.45565(10)	P44/R37	72/80	0.43	2686.80545(12)	P39/R37	35/42	0.34
2101.615464(94)	P40/R37	50/52	0.28	2692.40656(12)	P50/R48	42/48	0.38
2101.97804(18)	P40/R37	56/61	0.65	2692.40721(26)	Q43	35/35	0.79
2101.97828(17)	P40/R37	51/59	0.60	2692.814711(44)	P81/R67	122/133	0.21
2102.35030(20)	P36/R27	35/37	0.48	2692.81552(17)	Q51	43/51	0.57
2102.37982(17)	P51/R33	60/68	0.65	2699.935440(61)	P59/R59	103/108	0.26
2102.37892(15)	P50/R39	66/74	0.62	2699.935356(77)	P51/R52	99/99	0.39
2102.424019(99)	P38/R34	55/59	0.35	2699.93494(12)	Q55	47/51	0.44
2102.72159(24)	P35/R30	37/41	0.46	2699.93453(19)	Q68	36/55	0.55
2114.581738(88)	P74/R38	67/75	0.38	2822.268568(52)	P92/R45	88/107	0.31
2115.292245(58)	P77/R47	80/88	0.31	2822.268531(78)	Q49	48/49	0.28
2115.292355(68)	P79/R44	81/87	0.31	2966.58698(23)	P30/R28	25/30	0.47
2115.335118(95)	P64/R57	74/76	0.38	2966.58981(41)	Q34	21/24	0.83
2115.335056(79)	P55/R50	67/73	0.30	3016.005788(34)	P52/R48	90/97	0.28
2126.614351(51)	P66/R45	64/74	0.22	3102.81689(32)	P7/R43	32/37	0.44
2127.86936(36)	P89/R63	48/54	0.34	3102.81891(31)	Q33	23/23	0.75
2127.8688(1)	P44/R43			3144.88881(23)	P36/R42	59/63	0.73
2128.25829(51)	P87/R52	40/45	0.34	3226.72375(15)	P54/R48	82/89	0.55
2128.83097(66)	P84/R59	36/43	0.45	3226.72415(13)	P58/R45	83/96	0.48
2128.8285(1)	P44/R42			3227.73725(15)	P57/R42	88/92	0.67
2141.25050(63)	P95/R78	53/53	0.28	3245.392955(86)	P62/R45	101/106	0.39
2141.2506(1)	P59/R59			3245.392433(76)	P59/R44	96/102	0.39
2141.25063(63)	P96/R80	52/52	0.30	3246.54465(23)	P28/R26	25/32	0.31
2239.83651(16)	P27/R24	35/52	0.39	3360.26959(15)	P42/R32	53/59	0.53
2239.83737(11)	P31/R29	41/42	0.30	3375.42732(17)	P42/R33	39/54	0.54
2240.98319(16)	P32/R30	53/58	0.41	3376.96231(39)	P18/R16	19/30	0.54
2250.241650(76)	P48/R50	93/95	0.31	3385.84892(23)	P54/R13	28/31	0.54
2250.241352(35)	P47/R50	84/96	0.14	3385.84606(11)	P54/R7	24/44	0.42

ues are plotted versus the line wavenumbers in Fig.4. Due to a lack of experimental information, many important parameters are absent in the preliminary sets of effective Hamiltonian obtained for the $^{15}N_2{}^{16}O$ species. As a result, the deviations of the measured positions from their predicted values range between -0.65 and 0.7 cm^{-1}, which are much worse than the main species $^{14}N_2{}^{16}O$ [9], and other two isotopologues $^{14}N^{15}N^{16}O$ and $^{15}N^{14}N^{16}O$ [12].

The present work considerably extends our knowledge about the high-resolution spectra of $^{15}N_2{}^{16}O$ isotopologue of nitrous oxide molecule. 29 new bands have been observed for the first time, especially the observations of $(0441)\leftarrow(0440)$ Γ-Γ band rising from the high angular quantum number vibrational state will much improve the important effective Hamiltonian parameters of $^{15}N_2{}^{16}O$ isotopologue. Finally, new global fittings of the effective Hamiltonian and dipole parameters benefiting from the considerable amount of new observations obtained recently by FTS [4, 8] and CRDS [5] technique should lead to a considerable decrease of the deviations between the calculations and measurements. This modeling work is in progress at IAO Tomsk.

Supplementary Materials: The deviations between the measured values and the values calculated with the fitted rovibrational parameters are available at the CJCP website alongside the main article.

V. ACKNOWLEDGMENTS

[1] H. Y. Ni, K. F. Song, V. I. Perevalov, S. A. Tashkun, A. W. Liu, L. Wang, and S. M. Hu, J. Mol. Spectrosc. **248**, 41 (2008).

[2] K. F. Song, A. W. Liu, H. Y. Ni, and S. M. Hu, J. Mol. Spectrosc. **255**, 24 (2009).

[3] C. Y. Wang, A. W. Liu, V. I. Perevalov, S. A. Tashkun, K. F. Song, and S. M. Hu, J. Mol. Spectrosc. **257**, 94 (2009).

[4] B. Gao, C. Y. Wang, Y. Lu, A. W. Liu, and S. M. Hu, J. Mol. Spectrosc. **259**, 20 (2010).

[5] K. F. Song, B. Gao, A. W. Liu, V. I. Perevalov, S. A. Tashkun, and S. M. Hu, J. Quant. Spectrosc. Radiat. Trans. **111**, 2370 (2010).

[6] C. Amiot, J. Mol. Spectrosc. **59**, 380 (1976).

[7] R. A. Toth, J. Mol. Spectrosc. **197**, 158 (1999).

[8] O. M. Lyulin, D. Jacquemart, N. Lacome, S. A. Tashkun, and V. I. Perevalov, J. Quant. Spectrosc. Radiat. Trans. **111**, 345 (2010).

[9] V. I. Perevalov, S. A. Tashkun, and J. L. Teffo, *Sixteenth Colloquium on High Resolution Molecular Spectroscopy*, Dijon (France), 6-10 Sept. 103 (1999).

[10] J. L. Teffo, V. I. Perevalov, and O. M. Lyulin, J. Mol. Spectrosc. **168**, 390 (1994) .

[11] S. A. Tashkun, V. I. Perevalov, R.V. Kochanov, A. W. Liu, and S. M. Hu, J. Quant. Spectrosc. Radiat. Trans. **111**, 1089 (2010).

[12] L. S. Rothman, I. E. Gordon, A. Barbe, D. Chris Benner, P. F. Bernath, M. Birk, V. Boudon, L. R. Brown, A. Campargue, J. P. Champion, K. Chance, L. H. Coudert, V. Dana, V. M. Devi, S. Fally, J. M. Flaud, R. R. Gamache, A. Goldman, D. Jacquemart, I. Kleiner, N. Lacome, W. J. Lafferty, J. Y. Mandin, S. T. Massie, S. N. Mikhailenko, C. E. Miller, N. Moazzen-Ahmadi, O. V. Naumenko, A. V. Nikitin, J. Orphal, V. I. Perevalov, A. Perrin, A. Predoi-Cross, C. P. Rinsland, M. Rotger, M. Šimečková, M. A. H. Smith, K. Sung, S. A. Tashkun, J. Tennyson, R. A. Toth, A. C. Vandaele, and J. Vander Auwera, J. Quant. Spectrosc. Radiat. Trans. **110**, 533 (2009).